EARTHQUAKE ENGINEERING AND STRUCTURAL DYNAMICS, VOL. 11, 415-426 (1983)

CLASSIFICATION AND RATING OF STRONG-MOTION EARTHQUAKE RECORDS

R. N. IYENGAR* AND K. C. PRODHAN†

Department of Civil Engineering, Indian Institute of Science, Bangalore, India

SUMMARY

Ninety-two strong-motion earthquake records from the California region, U.S.A., have been statistically studied using principal component analysis in terms of twelve important standardized strong-motion characteristics. The first two principal components account for about 57 per cent of the total variance. Based on these two components the earthquake records are classified into nine groups in a two-dimensional principal component plane. Also a unidimensional engineering rating scale is proposed. The procedure can be used as an objective approach for classifying and rating future earthquakes.

INTRODUCTION

The rating of strong-motion earthquake records from an engineering point of view has been of interest for a long time. A variety of approaches have been suggested in the past for this purpose. The M.M. intensity scale is widely used when instrumental recordings are not available. This scale is subjective and hence imprecise. There are several ways of quantifying earthquakes. The Richter's magnitude is a measure of the energy released at the source. For the engineer this is only one of the important characteristics of an earthquake since it is the local ground acceleration which controls the response of structures. The peak ground acceleration, velocity and displacement have been individually and in combination suggested as indicators of seismic risk by many investigators.[2-4] This approach ignores the duration of the strong motion which would be important in assessing the safety of inelastic structures. The r.m.s. acceleration level as an indicator[5] includes the effect of the duration but overlooks other possible important parameters such as frequency content and site conditions. The response spectra are very good descriptors of structural response. Spectrum intensity[6] has been used in the literature as a simple indicator to compare earthquake records. But widely differing accelerograms can have spectrum intensities of the same order of magnitude. This is to some extent accounted for in Poceski's[7] definition of intensity, which combines the average velocity response and the r.m.s. ground velocity. The destruction causing potential of an earthquake is dependent on several characteristics. To search an indicator purely in terms of peak amplitudes or response values is limited in scope. In the literature itself there have been several attempts to understand the effects of other important parameters such as magnitude, epicentral distance and soil condition. Since these parameters may themselves be interrelated, the study of the variation of one isolated parameter with respect to some other isolated parameter will not be very appropriate. In other words what is necessary is to identify all the possible important parameters which contribute to the destruction potential and then to conduct a multivariate statistical analysis. With this in view, an attempt is made in this paper to analyse statistically the data of ninety-two earthquakes from California, U.S.A.

DATA

The basic data available from the U.S.A. have been documented in the EERL reports of the California Institute of Technology. Ninety-two site recordings have been selected from these reports for the present

---

* Associate Professor.
† Research Scholar.

0098-8847/83/030415-12$01.20

Received 12 April 1982
Revised 14 September 1982

study. For every site twelve parameters have been identified as important descriptors of damage potential. These are: (i) Richter's magnitude; (ii) duration in seconds; (iii) peak horizontal ground acceleration in cm/s^2 (a_p); (iv) peak horizontal ground velocity in cm/s; (v) peak horizontal ground displacement in centimetres; (vi) time to peak horizontal acceleration in seconds; (vii) ratio of the peak of the other horizontal component to a_p; (viii) ratio of the peak vertical acceleration to a_p; (ix) epicentral distance in kilometres; (x) soil condition; (xi) maximum of the pseudo relative velocity response spectra in cm/s; (xii) rate of zero crossing of the dominant horizontal component. The durations of strong motions used are the ones calculated by Trifunac and Brady.[8] The soil condition of every site is represented by a number in a three point scale as done by Trifunac.[9] Soft soil is indicated by 1. Medium soil conditions and hard rock are represented by 2 and 3 respectively. The twelfth parameter, namely, the rate of zero crossing has been counted from the standard records directly. This is included in the study since it is an important indicator of the dominant frequency of the accelerogram.[10] The complete set of data used in the analysis is presented in Appendix I.

PRINCIPAL COMPONENT ANALYSIS

Since in the present study, twelve parameters are considered important for a given accelerogram, in effect an earthquake is represented as a point in a twelve-dimensional space. However, from a statistical viewpoint, the twelve parameters are expected to be correlated. Hence it should be possible to reduce the dimensionality required to specify an earthquake profile and get a more parsimonious description which is maximally powerful in distinguishing the various profiles by applying principal component analysis.[11] The jth co-ordinate of the ith earthquake in the twelve-dimensional parameter space can be expressed as

$$E_{ij} = \sum_{n=1}^{12} P_{in} Q_{nj}; \quad i = 1, 2, \ldots, N; \quad j = 1, 2, \ldots, 12 \tag{1}$$

Q_{nj} are the eigenvectors of the correlation matrix

$$r_{kl} = \sum_{i} \bar{E}_{ik} \bar{E}_{il}; \quad k = 1, 2, \ldots, 12; \quad l = 1, 2, \ldots, 12 \tag{2}$$

where $\bar{E}_{ik}$ is the standardized non-dimensional random variable defined as

$$\bar{E}_{ik} = (E_{ik} - m_k)/s_k \tag{3}$$

$$m_k = (1/N) \sum_{i=1}^{N} E_{ik} \tag{4}$$

$$s_k^2 = [1/(N-1)] \sum_{i=1}^{N} [E_{ik} - m_k]^2 \tag{5}$$

The eigenvectors Q_{nj} are orthonormal and the subscripts n are arranged in the decreasing order of the eigenvalues so that Q_{1j} corresponds to the largest eigenvalue λ_1 and Q_{kj} corresponds to the kth largest eigenvalue λ_k. The kth principal component P_{ik} of the ith earthquake is defined as the dot product of the vectors $\bar{E}_{ij}$ and Q_{kj}. The total variance accounted for by the kth principal component is

$$v_k = \lambda_k \Big/ \sum_{l=1}^{12} \lambda_l \tag{6}$$

NUMERICAL RESULTS

The correlation matrix r_{kl} of the data considered is given in equation (7). On applying principal component analysis it is found that the first three eigenvalues are $\lambda_1 = 3{\cdot}825$, $\lambda_2 = 3{\cdot}001$ and $\lambda_3 = 1{\cdot}478$. These explain respectively 31·88 per cent, 25·01 per cent and 12·32 per cent of the total variance. In Table I, the mean and standard deviations of the twelve parameters are presented along with the first three eigenvectors. It is to be

$$
[r_{kl}] = \begin{bmatrix}
1{\cdot}0 & & & & & & & & & & & \\
0{\cdot}395 & 1{\cdot}0 & & & & & & & & & & \\
0{\cdot}182 & -0{\cdot}331 & 1{\cdot}0 & & & & & & & & & \\
0{\cdot}270 & -0{\cdot}177 & 0{\cdot}930 & 1{\cdot}0 & & & & \text{symmetric} & & & & \\
0{\cdot}348 & -0{\cdot}073 & 0{\cdot}751 & 0{\cdot}888 & 1{\cdot}0 & & & & & & & \\
0{\cdot}457 & 0{\cdot}481 & -0{\cdot}030 & 0{\cdot}038 & 0{\cdot}079 & 1{\cdot}0 & & & & & & \\
0{\cdot}158 & 0{\cdot}148 & -0{\cdot}040 & -0{\cdot}052 & 0{\cdot}004 & 0{\cdot}139 & 1{\cdot}0 & & & & & \\
0{\cdot}096 & -0{\cdot}060 & -0{\cdot}066 & 0{\cdot}029 & 0{\cdot}218 & -0{\cdot}037 & 0{\cdot}229 & 1{\cdot}0 & & & & \\
0{\cdot}410 & 0{\cdot}586 & -0{\cdot}343 & -0{\cdot}246 & -0{\cdot}178 & 0{\cdot}559 & 0{\cdot}204 & 0{\cdot}067 & 1{\cdot}0 & & & \\
-0{\cdot}154 & -0{\cdot}456 & 0{\cdot}237 & 0{\cdot}141 & 0{\cdot}006 & -0{\cdot}259 & 0{\cdot}042 & 0{\cdot}078 & -0{\cdot}222 & 1{\cdot}0 & & \\
0{\cdot}472 & -0{\cdot}04\,[\text{illegible}] & 0{\cdot}797 & 0{\cdot}852 & 0{\cdot}774 & 0{\cdot}157 & -0{\cdot}068 & -0{\cdot}056 & -0{\cdot}248 & -0{\cdot}013 & 1{\cdot}0 & \\
-0{\cdot}101 & -0{\cdot}490 & 0{\cdot}207 & 0{\cdot}050 & 0{\cdot}043 & -0{\cdot}370 & 0{\cdot}099 & 0{\cdot}231 & -0{\cdot}459 & 0{\cdot}389 & -0{\cdot}024 & 1{\cdot}0
\end{bmatrix} \quad (7)
$$

Table 1. Mean and standard deviation of the parameters and the first three eigenvectors of the correlation matrix

No. k	Parameter	Mean m_k	Std. deviation s_k	Q_{1j}	Q_{2j}	Q_{3j}
1	Magnitude	5·876	0·868	0·121	0·411	0·217
2	Duration; s	20·282	13·271	−0·194	0·432	−0·023
3	Peak horiz. acc., a_p; cm . s^{-2}	113·615	140·465	0·480	0·027	−0·055
4	Peak horiz. vel.; cm . s^{-1}	10·088	13·508	0·482	0·124	−0·050
5	Peak horiz. displ.; cm	4·370	5·521	0·438	0·174	0·064
6	Time to peak acc., a_p; s	5·395	5·747	−0·055	0·440	0·054
7	Other peak horiz. acc./a_p	0·703	0·174	−0·039	0·100	0·570
8	Peak vert. acc./a_p	0·478	0·219	0·034	−0·013	0·608
9	Epicentral dist.; km	58·741	56·625	−0·235	0·392	0·172
10	Soil condition	1·467	0·654	0·131	−0·285	0·255
11	Max. P.S.V.; cm . s^{-1}	69·831	64·390	0·441	0·207	−0·111
12	Zero crossing rate; s^{-1}	7·174	3·060	0·141	−0·343	0·372

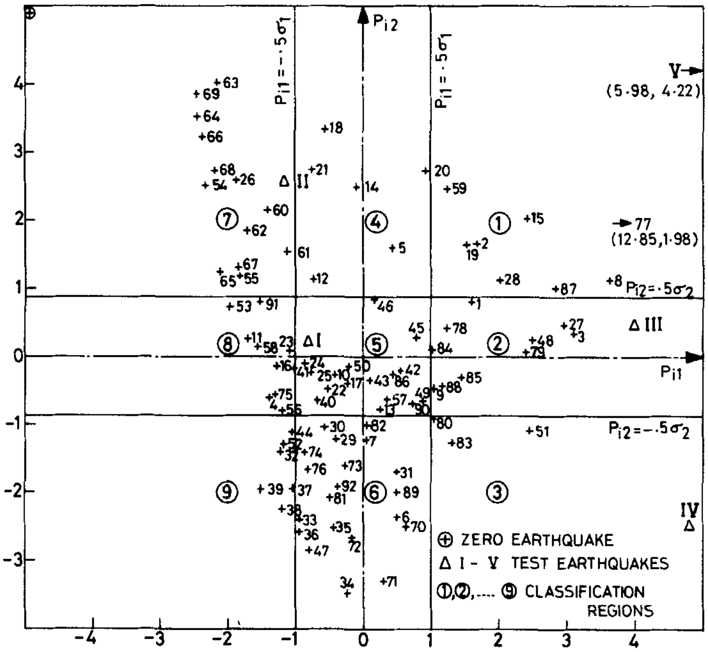

Figure 1. Principal component classification diagram

noted that the mean and standard deviations have the same units as the parameters but the elements of the eigenvectors are dimensionless. Once the twelve eigenvectors are known, all the twelve principal components of any earthquake can be found.

It may be noted that the principal component analysis is essentially a linear transformation procedure and one can consider an earthquake to be represented by the twelve new co-ordinates P_{ik} instead of the original $\bar{E}_{ik}$. However, since the first two components together explain 57 per cent of the variance, one can economically represent an earthquake in the two-dimensional space $P_{i1} - P_{i2}$. In Figure 1 this representation is shown for all the ninety-two earthquakes of the data set. The numbers shown are the serial numbers of the data set. It would be of interest to see whether some physical parameters could be associated with the new co-ordinates P_{i1} and P_{i2}. From Table I it is seen that the first eigenvector has significant positive values for maximum ground amplitudes and spectral velocity, and negative values for epicentral distance and duration. Since these quantities are like weights in finding the new co-ordinates P_{i1}, the first principal component stands for the amplitude–epicentral distance contrast. Similarly one can interpret P_{i2} to be the source strength–site condition contrast. It is to be observed that the zero crossing rate of an accelerogram is a good indicator of the site condition. This is brought out by the eigenvector Q_{2j} also, which has significant negative values for both these parameters. Figure 1 shows that the earthquakes are somewhat concentrated near the origin but no strong clustering tendency is observable. There is a tendency for the destructive earthquakes to have large P_1 values. In fact the El Centro 1940 earthquake has co-ordinates (3·63, 1·13) and the Pacoima Dam earthquake of 1971 has co-ordinates (12·85, 1·98).

CLASSIFICATION

If Figure 1 is taken as a standard reference diagram, one can mark future earthquakes on the same figure to get a comparison with known past earthquakes. For this purpose a simple division of the $P_{i1}-P_{i2}$ plane would be useful. Here this is done by drawing the lines $P_{i1} = \pm 0{\cdot}5\sigma_1$ and $P_{i2} = \pm 0{\cdot}5\sigma_2$, where σ_1 and σ_2 are the standard deviations of the variables P_{i1} and P_{i2} calculated with a sample size of $N = 92$. This approach automatically leads to a nine-way classification of the earthquakes as shown in Figure 1. Now, an examination of the various earthquakes region-wise brings out several interesting features of the present analysis. Regions 1, 2 and 3 contain high amplitude earthquakes, whereas regions 4, 5 and 6 consist of moderate amplitude earthquakes. Low amplitude records fall in the regions 7, 8 and 9. On the other hand, records from soil type 3 and soil type 2 will have negative P_{i2} due to their high frequency content. Thus regions 3, 6 and 9 are most likely to contain high frequency content records of short duration on hard rock sites. Regions 1, 4 and 7 are likely to represent low frequency shocks of long duration on soft soils.

At this stage, as a check, it would be interesting to see how earthquakes which were not included in the study would get marked on the classification diagram. For this purpose five earthquakes shown in Table II[12–15] have been selected. Firstly, the parameters of the earthquake are standardized with respect to the reference mean and standard deviation given in Table I. In the next step the dot product between the data vector and the reference eigenvectors Q_{1j} and Q_{2j} of Table I leads to the co-ordinates (P_1, P_2) of the new earthquakes. These are marked on the classification diagram of Figure 1. The location indicates how these earthquakes compare with the earthquakes of the data set.

Table II. Results for test earthquakes

Test earthquake no.	I	II	III	IV	V
Name of earthquake and recording station	9 February 1941, N-W Calif., Fernandale City Hall	9 February 1956, Alamo, Baja, Calif. El Centro	23 December 1972, Managua, South America, Esso Bld.	11 December, 1967, Koyna, India	12 June 1978, Miyagi-Oki Japan, Tohoku Univ.
Magnitude	6·4	6·8	6·2	6·3	7·4
Duration; s	20·82	50·42	16·5	6·1	20·0
Peak acc., a_p; cm.s^{-2}	61·3	50·1	351·0	618·03	259·23
Peak vel.; cm.s^{-1}	3·5	7·0	37·7	24·19	36·17
Peak displ.; cm	2·0	4·1	14·9	13·3	14·53
Time to peak acc.; s	5·42	6·8	6·26	4·12	7·56
Other peak horiz. acc./a_p	0·628	0·647	0·907	0·778	0·781
Peak vert. acc./a_p	0·313	0·248	0·854	0·54	0·59
Epicentral dist.; km	98·4	125·9	5·0	10·0	110·0
Soil condition	2·0	1·0	2·0	3·0	1·0
Max. P.S.V.; cm.s^{-1}	45·72	81·28	198·7	116·98	750·0
Zero crossing rate; s^{-1}	5·7	3·39	8·2	23·5	4·4
P_1	0·821	−1·153	4·011	4·806	5·975
P_2	0·181	2·554	0·483	−2·525	4·217
R	4·123	3·791	8·956	9·751	10·92
Actual site MMI	6	6	6	8	8
Predicted site MMI (authors)	5·57	5·16	9·36	9·77	10·33

DAMAGEABILITY AND RATING SCALE

In Figure 1 the earthquakes are marked relatively and hence comparison can be made only with respect to another earthquake and not with respect to an absolute point. But for understanding the dependence between damage potential and the principal components it would be necessary to fix up on the diagram, the zero-damage-causing earthquake. This can be done by considering an imaginary earthquake data which would cause no damage at a given site. For example, one can choose the following data vector for the zero earthquake:

$$\{m_1,\ 0, 0, 0, 0, 0, 1, 1, 15m_9, m_{10}, 0, 0\}$$

This assumes that a 5·88 magnitude earthquake will not produce any strong motion and damage at a distance of 881 km. The co-ordinates of this earthquake in the $P_{i1}-P_{i2}$ plane (Figure 1) are (−4·9445, 5·0547). If the magnitude is changed to 9·0, keeping other values constant, the co-ordinates will be (−4·505, 6·5313). Thus it is seen that if increase in magnitude means increased damage, it will be associated with an increase in the first principal component P_1. A similar tendency has been found to exist if epicentral distance is reduced, holding all other parameters constant. This leads one to postulate that the distance of a strong motion earthquake from the zero earthquake in the first principal component direction would be a good measure of its damage-causing potential. Thus $R = P_1 + 4{\cdot}9445$ is proposed as a scale for risk rating of earthquakes. This hypothesis can be verified only by comparing the risk rating R_i of the earthquakes of the data set with the historical damages caused by them. The most popular way of damage assessment at a site has been in terms of MMI site intensities. Figure 2 shows the relationship between R_i and MMI of the ninety-two data earthquakes. Even though there is a large scatter in the data, there seems to be a trend of increase in

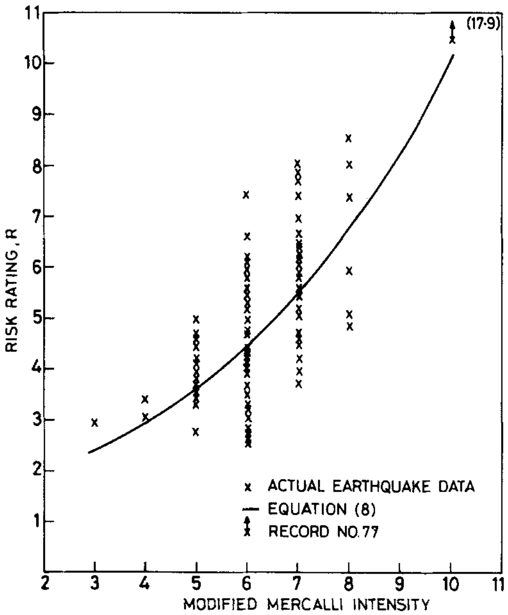

Figure 2. Dependence of risk rating, R, on MMI

R with increase in MMI. To verify the statistical significance of this trend, the correlation coefficient between $\log R$ and MMI has been calculated. This value is found to be 0·6468 which is highly significant as verified by the standard T-test. With this in the background, the empirical relationship

$$R = 1{\cdot}315\, e^{0{\cdot}205\,\mathrm{MMI}} \tag{8}$$

is proposed as a least square fit between R and MMI. This curve is also shown in Figure 2. It has to be kept in mind that R is a continuous variable whereas MMI is generally specified as an integer. At this stage it would be interesting to see how well the site intensities are predictable once the rating R is known. In Table 2 for the five test earthquakes the predicted and the observed site intensities are compared. Comparison seems favourable, particularly in view of the uncertainties involved in the data.

DISCUSSION

The present study aims at developing a classification diagram and an objective rating scale for earthquakes. This is achieved by conducting a principal component analysis on twelve most important parameters associated with a large number of earthquakes. Even though correlation studies have been attempted previously they are not comprehensive since the number of parameters considered has been small. Even with twelve parameters, as in the present analysis, it is seen that the variance explained by the first two principal components is only 75 per cent. Naturally, the question arises as to what could be the other parameters to be included in describing an earthquake. Probably, focal depth, r.m.s. value of the acceleration history and r.m.s. spectrum level are some of the other important parameters. The more crucial question is on the unbiasedness or otherwise of the data and the dependence of the results on the population size. An element of bias in the data included is unavoidable, since, to date, a large number of strong-motion records have come only from California, U.S.A. However, bias towards a single event, namely, the 9 February 1971 San Fernando earthquake, has been avoided by not including all the site recordings available for this event alone. The effect of the population size has been investigated to some extent. In Table III the dependence of m_k and s_k $(k = 1, 12)$ on the size of the data is shown for various values of N. Figure 3 shows the dependence of Q_{kj} on N. It may be observed that the convergence of the results is fast and hence the classification of Figure 1 may be taken as reasonably stable.

Table III. Convergence of mean and standard deviation

	m_k					s_k				
Parameters	$N = 50$	$N = 60$	$N = 70$	$N = 80$	$N = 92$	$N = 50$	$N = 60$	$N = 70$	$N = 80$	$N = 92$
Magnitude	5·680	5·713	5·797	5·798	5·876	1·073	0·997	0·951	0·905	0·868
Duration; s	19·208	21·110	22·557	21·169	20·282	11·156	13·397	13·958	13·706	13·271
Peak horiz. acc., a_p; cm . s^{-2}	114·592	109·193	98·620	111·943	113·615	90·96	95·253	94·149	148·544	140·465
Peak horiz. vel.; cm . s^{-1}	10·100	9·708	8·874	10·040	10·088	8·568	8·650	8·299	14·206	13·508
Peak horiz. displ.; cm	4·364	4·168	3·860	4·398	4·370	4·791	4·600	4·333	5·778	5·521
Time to peak acc.; s	4·892	4·956	6·137	5·671	5·395	4·762	4·551	6·256	6·036	5·747
Other peak horiz. acc./a_p	0·747	0·751	0·762	0·767	0·763	0·190	0·188	0·182	0·177	0·174
Peak vert. acc./a_p	0·434	0·429	0·446	0·461	0·478	0·226	0·214	0·225	0·223	0·219
Epicentral dist. km	37·700	45·368	64·070	60·298	58·741	30·158	37·455	62·393	59·401	56·625
Soil condition	1·320	1·35	1·343	1·388	1·467	0·513	0·547	0·535	0·584	0·654
Max. P.S.V.; cm . s^{-1}	76·582	72·395	66·059	67·906	69·831	59·029	58·908	56·835	65·642	64·390
Zero crossing rate; s^{-1}	6·595	6·442	6·206	6·774	7·174	2·300	2·238	2·445	2·891	3·060

CONCLUSIONS

The statistical classification and rating scale developed in the present analysis can be used as an objective approach for understanding the damageability of strong-motion earthquakes. The study includes the effects of the twelve most important parameters in arriving at the final results. Once these parameters are known or

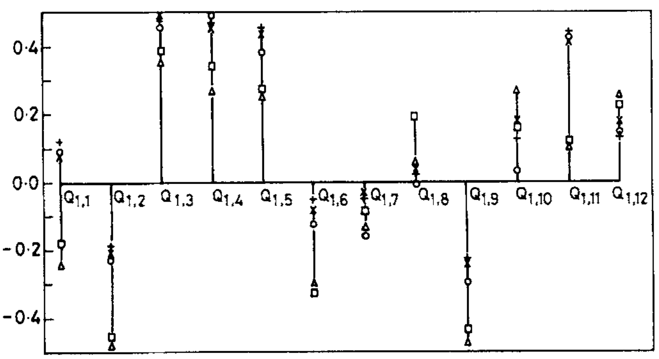

Figure 3(a). Convergence of vector Q_{1j} with population size, N

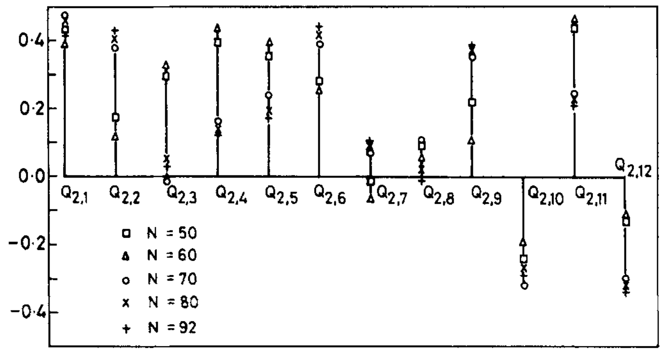

Figure 3(b). Convergence of vector Q_{2j} with population size, N

are estimated for a real or an artificial earthquake, the position of the shock in the classification diagram is fixed. This position directly gives a comparison between the given earthquake and past records used in the data set. Thus, one can find the nearest past earthquake and use this information in design and analysis. Alternatively one can from postulated MMI values estimate the risk rating R from Figure 2. This fixes the first principal component P_{i1} of the earthquake. If, now from other information one can specify eleven of the twelve parameters, the unknown parameter can be estimated easily. This approach may be conveniently used to fix up the peak of the undamped pseudo-velocity spectrum at a given site. Also one can define typical earthquakes of the nine classification regions by averaging the data in the regions. This, of course, calls for more data. In this connection it would be useful to find whether typical response spectra can also be defined for the classification regions. Also one can improve upon the analysis by including more parameters which describe ground motion and structural response.

ACKNOWLEDGEMENTS

Professor G. W. Housner sent several of the EERL reports used in the study. Professor M. D. Trifunac made available data on duration, epicentral distance and site intensities used in his studies. Thanks are due to these two persons for their help.

APPENDIX I

Sl. no.	EERL record no. (1)	Mag. (2)	Duration s (3)	Peak horiz. acc., a_p; cm . s^{-2} (4)	Peak horiz. vel.; cm . s^{-1} (5)	Peak horiz. displ.; cm (6)	Time to a_p; s (7)	Other peak horiz. acc./a_p (8)	Peak vert. acc./a_p (9)	Epi. dist.; km (10)	Soil cond. (11)	Max. P.S.V.; cm . s^{-1} (12)	Zero crossing rate; s^{-1} (13)	Site MMI (14)
1	B021	6·3	21·56	151·0	17·3	17·5	2·14	0·862	0·987	47·8	1·0	88·90	6·20	6
2	V314	6·3	24·02	95·6	23·7	16·3	7·50	0·652	0·665	54·9	1·0	142·24	4·20	7
3	V315	6·3	8·34	192·7	29·4	22·7	2·98	0·810	1·452	27·2	1·0	100·33	8·10	8
4	B023	5·4	19·76	32·1	2·0	0·8	0·12	0·822	0·333	38·4	1·0	18·42	4·40	5
5	B024	6·5	21·24	179·1	11·6	3·7	15·12	0·875	0·380	60·8	1·0	132·08	6·89	6
6	B025	6·0	2·16	143·5	7·3	1·4	3·04	0·993	0·610	6·6	3·0	34·29	11·82	7
7	B026	5·5	10·22	140·9	6·6	3·9	2·26	0·618	0·224	55·3	2·0	46·99	7·67	6
8	A001	6·7	24·44	341·7	33·4	10·9	2·12	0·615	0·604	9·3	1·0	254·00	6·93	8
9	U299	5·9	4·56	233·8	21·8	3·7	0·24	0·737	0·250	35·9	1·0	81·28	5·02	8
10	V316	5·4	11·96	53·7	9·3	3·6	8·88	0·739	0.158	6·2	1·0	46·99	5·25	6
11	V317	5·4	35·80	14·9	1·3	0·8	9·08	0·752	0·450	28·5	1·0	8·67	6·20	6
12	T286	6·5	51·88	58·5	6·2	4·2	2·82	0·795	0·431	46·5	1·0	68·58	7·85	6
13	U301	5·3	9·84	193·6	11·7	1·4	4·22	0·617	0·359	29·3	1·0	78·74	6·83	7
14	B028	7·1	41·02	66·5	8·2	2·4	10·46	0·991	0·331	57·8	1·0	177·80	4·8	8
15	B029	7·1	18·02	274·6	17·1	10·4	19·62	0·589	0·330	16·8	1·0	208·28	8·20	8
16	T287	5·6	33·94	30·4	3·0	2·0	1·16	0·908	0·438	27·5	1·0	27·94	6·50	6
17	A002	5·8	16·94	109·5	7·4	2·7	4·38	0·932	0·241	56·3	2·0	60·96	6·36	5
18	A003	7·7	29·62	52·1	9·1	2·9	16·70	0·890	0·562	126·0	1·0	127·00	3·27	7
19	A004	7·7	29·00	175·9	17·7	9·2	3·7	0·868	0·585	43·0	1·0	152·40	7·23	7
20	A005	7·7	33·70	128·6	19·3	5·8	6·98	0·683	0·339	89·5	1·0	187·96	3·46	7
21	A006	7·7	32·12	54·1	6·1	5·1	13·28	0·804	0·416	119·5	1·0	71·12	4·84	7
22	B030	5·5	18·48	74·1	4·7	1·9	5·10	0·717	0·394	43·2	2·0	66·04	4·75	6
23	T288	5·5	40·62	35·8	6·3	1·5	7·56	0·201	0·472	23·6	1·0	40·64	7·05	5
24	B031	5·9	16·38	66·8	3·7	1·1	6·40	0·957	0·531	43·0	1·0	38·10	7·20	6
25	U305	5·3	21·92	52·0	4·2	2·2	4·00	0·940	0·444	36·2	1·0	66·04	6·60	6
26	T289	6·3	43·00	27·0	3·2	2·7	15·20	0·896	0·248	149·8	1·0	38·10	5·25	4
27	A008	6·5	10·00	252·7	29·4	14·1	3·84	0·651	0·332	24·0	2·0	165·10	4·43	7
28	A009	6·5	19·52	197·3	26·0	9·6	7·10	0·789	0·212	40·4	2·0	172·72	3·60	7
29	A010	5·8	10·12	105·8	4·4	1·7	1·20	0·947	0·418	9·8	1·0	27·94	9·20	7
30	T292	5·4	19·78	71·1	5·2	2·2	0·00	0·872	0·795	23·5	1·0	35·56	8·80	6
31	V329	4·7	4·70	163·6	17·9	4·0	0·24	0·531	0·151	5·4	1·0	49·02	6·60	6

Appendix I (*cont.*)

Sl. no.	EERL record no. (1)	Mag. (2)	Duration s (3)	Peak horiz. acc., a_p; cm . s^{-2} (4)	Peak horiz. vel.; cm . s^{-1} (5)	Peak horiz. displ.; cm (6)	Time to a_p; s (7)	Other peak horiz. acc./a_p (8)	Peak vert. acc./a_p (9)	Epi. dist.; km (10)	Soil cond. (11)	Max. P.S.V.; cm . s^{-1} (12)	Zero crossing rate; s^{-1} (13)	Site MMI (14)
32	A013	3·8	16·62	45·9	2·9	1·1	1·76	0·978	0·584	16·8	1·0	35·56	5·10	7
33	A014	3·8	9·76	45·4	2·1	1·0	2·04	0·921	0·661	15·2	2·0	21·59	7·37	7
34	A015	3·8	2·80	102·8	4·6	0·8	1·44	0·796	0·362	11·8	2·0	26·67	13·92	7
35	A016	3·8	5·56	83·8	5·1	1·1	1·80	0·658	0·529	14·6	2·0	48·26	6·90	7
36	A017	3·8	11·68	39·0	2·0	1·5	0·48	0·610	0·392	24·3	2·0	16·51	7·30	6
37	V322	4·4	10·56	24·6	2·6	1·2	1·26	0·350	0·248	17·3	2·0	25·40	3·20	5
38	V323	4·4	7·96	18·6	1·0	0·7	0·02	0·844	0·312	15·6	2·0	5·84	5·80	5
39	V328	4·0	12·98	9·0	0·9	0·5	0·60	0·233	0·311	18·3	1·0	4·70	4·00	5
40	U307	5·0	27·80	55·5	5·3	1·9	1·06	0·636	0·425	8·5	1·0	71·12	5·70	6
41	U308	5·7	25·66	73·6	3·6	1·2	7·08	0·783	0·196	60·3	2·0	29·21	6·39	6
42	A018	5·7	16·60	175·7	17·1	3·8	1·20	0·361	0·279	40·0	1·0	93·98	4·50	7
43	U309	5·7	16·46	168·6	10·8	3·0	0·00	0·444	0·357	40·0	1·0	78·74	3·90	7
44	V330	5·0	18·86	47·3	2·7	1·2	4·30	0·958	0·275	19·0	2·0	25·91	6·14	6
45	B032	6·5	21·16	194·3	13·1	3·8	6·42	0·681	0·308	61·1	1·0	116·84	11·45	7
46	U310	6·5	20·12	77·6	9·4	5·4	9·96	0·673	0·414	22·3	1·0	96·52	5·40	8
47	V331	4·0	5·08	40·4	2·1	0·9	0·22	0·889	0·651	14·9	2·0	15·75	9·33	5
48	B034	5·6	6·78	425·7	25·4	7·1	7·50	0·817	0·275	32·4	1·0	157·48	6·81	6
49	B035	5·6	11·10	269·6	11·8	3·9	4·54	0·863	0·288	34·1	1·0	86·36	10·20	6
50	B036	5·6	28·22	63·2	8·0	5·7	5·46	0·824	0·706	36·5	1·0	58·42	10·66	6
51	B037	5·6	4·48	340·8	22·5	5·5	4·30	0·776	0·381	31·0	3·0	152·40	6·80	7
52	B038	5·6	19·06	14·2	1·1	1·2	0·48	0·803	0·430	76·1	2·0	8·38	9·60	5
53	U311	5·4	33·28	11·2	2·2	1·5	1·76	0·723	0·536	130·5	1·0	22·86	3·00	3
54	T293	6·3	66·54	14·8	2·4	1·7	5·84	0·912	0·331	148·1	1·0	30·48	5·65	6
55	V332	6·3	18·86	14·5	1·6	0·7	10·78	0·862	0·559	151·5	1·0	11·94	6·20	6
56	B039	5·8	19·98	20·8	2·3	0·9	0·88	0·938	0·370	50·6	2·0	11·68	5·90	5
57	U312	5·8	16·58	232·1	11·9	1·7	6·60	0·444	0·140	30·6	2·0	52·07	6·00	6
58	U313	5·2	35·80	16·3	1·7	2·1	5·04	0·804	0·613	39·0	1·0	19·05	4·90	5
59	A019	6·4	49·30	127·8	25·8	12·2	8·54	0·441	0·232	69·8	1·0	157·48	5·06	6
60	A020	6·4	42·28	29·5	6·0	4·4	8·54	0·980	0·424	109·9	1·0	48·26	3·68	6
61	B040	6·4	30·02	45·5	4·2	2·9	15·86	0·879	1·191	134·4	2·0	34·29	6·40	5
62	Y370	6·4	27·10	28·1	2·7	2·1	14·14	0·765	0·765	146·2	1·0	22·35	5·43	6

Appendix I (*cont.*)

Sl. no.	EERL record no. (1)	Mag. (2)	Duration; s (3)	Peak horiz. acc., a_p; cm . s^{-2} (4)	Peak horiz. vel.; cm . s^{-1} (5)	Peak horiz. displ.; cm (6)	Time to a_p; s (7)	Other peak horiz. acc./a_p (8)	Peak vert. acc./a_p (9)	Epi. dist.; km (10)	Soil cond. (11)	Max. P.S.V.; cm . s^{-1} (12)	Zero crossing rate; s^{-1} (13)	Site MMI (14)
63	Y371	6·4	53·18	13·2	4·4	3·5	24·40	0·886	0·487	173·1	1·0	41·91	3·90	5
64	Y372	6·4	44·10	9·5	2·9	2·1	20·58	0·916	0·537	205·1	1·0	15·88	4·00	6
65	Y373	6·4	26·22	7·4	1·4	0·5	3·12	0·946	0·662	220·3	2·0	11·68	3·70	6
66	Y376	6·4	34·08	11·1	2·5	1·6	20·90	0·693	0·376	212·0	1·0	20·33	3·30	6
67	Y378	6·4	17·06	11·7	3·1	2·3	1·32	0·598	0·462	218·8	1·0	22·86	2·60	6
68	Y379	6·4	47·20	18·5	4·7	2·7	3·24	1·000	0·378	212·2	1·0	36·83	2·70	6
69	Y380	6·4	30·82	12·4	3·2	1·4	26·60	0·879	0·387	227·3	1·0	25·40	2·60	6
70	W334	5·4	2·64	194·4	9·6	1·0	2·08	0·715	0·273	13·4	2·0	48·89	13·26	6
71	W335	5·4	5·30	69·9	5·6	2·4	0·66	0·785	0·848	19·2	3·0	17·78	16·00	6
72	W336	5·4	3·04	69·4	4·0	1·2	0·78	0·807	0·532	22·4	2·0	19·05	13·70	6
73	W338	5·4	8·76	113·8	4·8	1·8	1·06	0·505	0·461	29·9	1·0	40·64	9·87	6
74	W339	5·4	10·60	40·2	2·6	0·9	0·04	0·881	0·836	31·5	1·0	21·59	8·70	6
75	W342	5·4	18·76	19·4	1·5	1·7	4·04	0·964	0·639	56·0	1·0	14·61	8·40	5
76	W344	5·4	12·04	24·1	2·0	2·4	1·48	0·602	0·639	58·9	2·0	13·97	9·00	5
77	C041	6·4	6·98	1148·1	113·2	37·7	7·74	0·919	0·606	9·1	3·0	381·00	9·70	10
78	C054	6·4	13·24	147·1	17·4	11·8	4·72	0·795	0·315	41·9	1·0	91·44	7·42	7
79	D058	6·4	13·26	207·0	21·1	14·7	3·36	0·808	0·420	37·1	1·0	139·7	12·10	7
80	E081	6·4	22·50	213·0	9·8	7·0	0·20	0·931	0·299	32·9	2·0	68·58	12·60	6
81	F102	6·4	8·34	24·6	1·4	0·8	0·18	0·837	0·622	68·5	3·0	12·19	12·40	5
82	F103	6·4	14·00	120·5	5·4	2·4	1·00	0·759	0·393	45·4	1·0	55·88	13·20	5
83	G106	6·4	6·22	188·6	11·6	5·0	5·78	0·464	0·443	36·1	3·0	88·90	9·00	7
84	G107	6·4	12·78	107·3	14·3	7·4	7·90	0·871	0·866	39·8	1·0	114·30	10·60	7
85	G110	6·4	9·64	207·8	13·9	5·0	5·10	0·669	0·608	31·5	2·0	137·16	7·00	7
86	G114	6·4	19·08	136·2	9·3	2·8	0·10	0·814	0·636	32·3	1·0	111·76	8·86	6
87	H115	6·4	18·46	220·6	28·2	13·5	6·96	0·662	0·428	29·3	1·0	198·12	8·40	7
88	J141	6·4	15·66	145·5	18·0	3·4	4·32	0·748	0·639	29·6	3·0	119·38	5·40	6
89	J143	6·4	10·48	119·3	4·8	2·0	2·22	0·917	0·599	26·6	3·0	53·34	13·60	6
90	L166	6·4	12·02	164·2	12·4	4·9	4·52	0·899	0·424	30·8	2·0	63·50	9·72	7
91	L171	6·4	36·50	15·9	2·8	2·1	4·16	0·755	0·648	139·8	2·0	19·05	6·07	4
92	M179	6·4	9·32	46·7	2·8	0·9	0·46	0·445	0·824	70·7	2·0	18·42	13·80	5

REFERENCES

1. H. O. Wood and F. Neumann, 'Modified Mercalli intensity scale of 1931', *Bull. seism. soc. Am.* **21**, 277–283 (1931).
2. M. D. Trifunac and A. G. Brady, 'On the correlation of seismic intensity scales with the peaks of recorded strong ground motion', *Bull. seism. soc. Am.* **65**, 139–162 (1975).
3. J. R. Murphy and L. J. O'Brien, 'The correlation of peak ground acceleration amplitude with seismic intensity and other physical parameters', *Bull. seism. soc. Am.* **67**, 877–915 (1977).
4. N. M. Newmark and E. Rosenblueth, *Fundamentals of Earthquake Engineering*, Prentice-Hall, Englewood Cliffs, N.J., 1971.
5. M. W. McCann Jr. and H. C. Shah, 'Determining strong motion duration of earthquakes', *Bull. seism. soc. Am.* **69**, 1253–1265 (1979).
6. G. W. Housner, 'Strong ground motion', in *Earthquake Engineering* (Ed. R. L. Wiegel), Prentice-Hall, Englewood Cliffs, N.J., 1970, pp. 89–90.
7. A. P. Poceski, 'An intensity definition of strong motion earthquakes', *Proc. 6th world conf. earthquake eng.*, New Delhi, 2.546–2.551 (1977).
8. M. D. Trifunac and A. G. Brady, 'A study on the duration of strong earthquake ground motion', *Bull. seism. soc. Am.* **65**, 581–626 (1975).
9. M. D. Trifunac, 'Preliminary analysis of the peaks of strong earthquake ground motion—dependence of peaks on earthquake magnitude, epicentral distance and recording site condition', *Bull. seism. soc. Am.* **66**, 189–219 (1976).
10. R. N. Iyengar and K. T. S. Iyengar, 'A non-stationary random process model for earthquake accelerograms', *Bull. seism. soc Am.* **59**, 1163–1188 (1969).
11. R. Gnanadesikan, *Methods for Statistical Data Analysis of Multivariate Observations*, Wiley, New York, 1977.
12. S. T. Algermissen *et al.*, 'The Managua, Nicaragua, earthquake of December 23, 1972: location, focal mechanism and intensity distribution', *Bull. seism. soc. Am.* **64**, 993–1004 (1974).
13. 'Recent seismic disturbances in the Shivajinagar Lake area of the Koyna Hydroelectric Project, Maharastra, India', Central Water Power Research Station, Khadakwasla, Poona, India, Jan. 1970.
14. 'An investigation of the Miyagi-Ken-Oki, Japan, earthquake of June 12, 1978, *NBS Special Publication 592*, National Bureau of Standards, Washington, DC, U.S.A. (1980).
15. K. Kubo, 'Effects of the Miyagi-Oki, Japan earthquake of June 12, 1978, on lifeline systems', *Proc. 2nd U.S. natl. conf. earthquake eng.*, Stanford, U.S.A. 343–362 (1979).